Radiocarbon, Vol 60, Nr 1, 2018, p 75–90 DOI:10.1017/RDC.2017.80

AGE CONSTRAINTS ON GULF OF MEXICO DEEP WATER VENTILATION AS DETERMINED BY ^{14}C MEASUREMENTS

Piers Chapman[1*] • Steven F DiMarco[1] • Robert M Key[2] • Connie Previti[1] • Shari Yvon-Lewis[1]

[1]Department of Oceanography, Texas A&M University, College Station, TX 77843-3146, USA.
[2]Program in Atmospheric and Oceanic Sciences, Princeton University, Princeton, NJ 08544, USA.

ABSTRACT. While the exchange of water through Yucatan Strait is reasonably well known, the age of the deep water in both the Caribbean Sea and Gulf of Mexico is not. We recently measured the radiocarbon (^{14}C) concentrations in deep water in the Gulf of Mexico from a line of stations along 90°30′W. The mean apparent age of water below 900 m, the depth of the Florida Strait sill, was found to be about 740 yr relative to the 1950 ^{14}C standard. Depending on how the corrections for biological activity in the upper water are applied, this converts to a "true" age of between 231 ± 28 and 293 ± 74 yr. These ages agree with a previous estimate of the age of the deep water in the Gulf of Mexico based on heat flows, put upper limits on the age of the deep water in the Caribbean Sea, and provide constraints on modelers for the return of deep water from the Gulf of Mexico to the Caribbean. This might be important in the event of a future deep water oil or other chemical spill in the region.

KEYWORDS: Gulf of Mexico, radiocarbon AMS dating, water.

INTRODUCTION

The Gulf of Mexico (henceforth GoM) is a flat-bottomed basin with a maximum depth near 3800 m. It is fed by Caribbean inflow through Yucatan Strait, over a sill about 2000 m deep. Water exits the GoM to the Atlantic Ocean, via Florida Strait over a 740-m-deep sill. Within the GoM, therefore, there is considerable shear between the upper layer circulation that includes tropical and subtropical waters and that below the Florida Strait sill depth (Morrison et al. 1983; Jochens et al. 2005). The Florida Strait sill depth coincides with the center of the Antarctic Intermediate Water (AAIW) layer. Water below about 1000 m is essentially well mixed with a constant salinity of 34.97 indicative of upper NADW (Schroeder et al. 1974; Morrison et al. 1983; Nowlin et al. 2001), as well as consistent with oxygen concentrations (Jochens et al. 2005). Nutrient concentrations, however, are less well constrained (Nowlin et al. 2001). Water masses identified in the GoM are listed in Table 1, together with their physico-chemical characteristics.

The GoM is characterized by an anticyclonic upper layer circulation that is forced by the Loop Current and a cyclonic circulation below 950–1000 m depth. Within the lower layer, current velocities drop from as high as 2.5 m/s in the Loop Current to approximately 10 cm/s or less at 1200 m, and are likely only 1–2 cm/s at greater depths (Schmitz 2005; Ledwell et al. 2016). The deep cyclonic circulation is inferred from both deep current meter and PALACE float measurements (Molinari and Mayer 1980; Hamilton 1990; Hamilton et al. 2003; Weatherly et al. 2005; Hamilton et al. 2016) and from hydrographic data. DeHann and Sturges (2005) showed that water temperatures increase slowly to the northeast around the edge of the basin at 2000 m as water moves away from Yucatan Strait with its cold, oxygen-rich inflow. Similarly, oxygen concentrations below 1200 m depth show the highest values near Yucatan Strait and decrease cyclonically around the basin so that the lowest values are found in the Bay of Campeche in the southwest GoM (Jochens et al. 2005). While this cyclonic circulation is found in both the eastern and western sub-basins of the GoM, recent float data suggest separate circulations may exist either side of 90°W (Hamilton et al. 2016), and remnants of the upper layer circulation can still be seen as deep as 2000 m in mean temperature plots from below the depth of the Florida Strait sill.

*Corresponding author. Email: piers.chapman@tamu.edu.

Table 1 Water masses of the Gulf of Mexico, based on (a) Morrison and Nowlin (1977), (b) Nowlin and McClellan (1967), and (c) Morrison et al. (1983).

Water mass	Depth (m)	Density ($kg.m^{-3}$)	Characteristics
Eastern Gulf of Mexico (a, b)			
SUW-LC	150–250	25.40	S_{max} 36.7–36.8
SUW	150–250	25.40	S_{max} 36.4–36.5
18°C water	200–400	26.50	O_{max} 160–170 $\mu mol.kg^{-1}$
TACW	400–700	27.15	O_{min} 125–145 $\mu mol.kg^{-1}$
AAIW	700–900	27.40	P_{max} 1.8–2.5 $\mu mol.kg^{-1}$
	800–1000	27.50	S_{min} 34.86–34.89
UNADW-MIX	900–1200	27.70	Si_{max} 23–25 $\mu mol.kg^{-1}$
UNADW	Below 1200	27.72–27.73	S ~34.97
Western Gulf of Mexico (b, c)			
SUW	0–250	25.40	S_{max} 36.4–36.5
TACW	250–400	27.15	O_{min} 110–130 $\mu mol.kg^{-1}$
AAIW	500–700	27.30	N_{max} 29-35 $\mu mol.kg^{-1}$
	600–800	27.40	P_{max} 1.7–2.5 $\mu mol.kg^{-1}$
	700–800	27.50	S_{min} 34.88-34.89
UNADW	Below 1200	27.72–27.73	

18°C water = 18°C Sargasso Sea water; AAIW = Antarctic intermediate water; SUW = Subtropical underwater; SUW-LC = subtropical underwater within the Loop Current; TACW = Tropical Atlantic Central water; UNADW = Upper North Atlantic deep water; UNADW-MIX = UNADW mixed with high silicate Caribbean mid-water.

The analysis of Johns et al. (2002) suggests that net northward flow through Yucatan Strait is ~28.5 Sv. This agrees reasonably well with model estimates of 29 Sv by Roemmich (1981), 27 Sv by Romanou et al. (2004) and 27.2 Sv by Cherubin et al. (2005). The CANEK program of direct current measurements, named after a prominent figure in local Mayan literature (Badan et al. 2005), however, gave a mean northward transport of only 23.8 ± 1 Sv over 9 months and 23.1 ± 3.1 Sv over 2 yr (Sheinbaum et al. 2002; Candela et al. 2003, Badan et al. 2005). CANEK researchers suggested that the 4–5 Sv discrepancy results from balancing flow in the Florida Current (east of Florida Strait) with poorly known flow through the Old Bahama and Northwest Providence Channels east of Cuba. There is, however, a large amount of sub-inertial variability in the current meter records. On the other hand, repeated ADCP measurements taken from a cruise liner over several years (Rousset and Beal 2010) suggest that the flows through Yucatan Strait and in the Florida Current are essentially equal at 30.3 ± 5 Sv and 30.8 ± 3.2 Sv respectively, while altimetry estimates (Alvera-Azcarate et al. 2009) give flow values through Florida Strait of 32.2 Sv over 13 yr. Clearly, some uncertainty remains over the absolute flows in the region.

The flow is not one way, however. LADCP data (Ochoa et al. 2001) and current meter records (Bunge et al. 2002; Sheinbaum et al. 2002; Candela et al. 2003) show considerable southward flow along the eastern and western sides of Yucatan Strait, both at the surface near Cuba (volume flux ~0.4 Sv) and at depth, where the flow is about 1.5 Sv, although they state that there is essentially no net mass transport below the depth of the Florida Strait sill. This is borne out by model results; Cherubin et al. (2005) showed a mean southward outflow between 3 and 4 Sv over a 7-yr model run. The flow variability is thought to be related to the formation of Loop Current eddies in the Gulf of Mexico (Maul et al. 1985; Bunge et al. 2002), although the exact mechanism is unclear (Cherubin et al. 2005). This outflow water carries up to 150 GW of heat back to the Caribbean below 750 m depth. An additional 110 GW of heat is lost via eddy heat flux. In exchange, colder, denser water with high oxygen concentrations near the sill depth ventilates the deep Gulf of Mexico (Rivas et al. 2005). The overall heat flux below 750 m depth is, however, strongly positive into the GoM at about 2900 GW.

Knowledge of the age of the deep water in the Gulf of Mexico is important for constraining models of the region. As a result of the two-layer circulation pattern, GoM deep water has a long turnover time, but this is not known with any certainty. The recent Deepwater Horizon oil spill in 2010 led to increased interest in modeling the circulation in the GoM, and age estimates put limits on the time needed to clear any future oil or other potential toxic agent from the Gulf.

Rivas et al. (2005) used calculations based on near-bottom heat and mass fluxes (estimated at about 0.32 Sv) to estimate a residence time of about 250 ± 50 yr. We recently obtained $\Delta^{14}C$ data that suggest a similar deep water mean age.

SAMPLING AND METHODOLOGY

Samples for $\Delta^{14}C$ analysis were collected during *Pelican* cruise PE15-21 (32PE20150414) from April 14–19, 2015, at sites shown in Figure 1, and are available from the Gulf Research Initiative Data Archive at https://data.gulfresearchinitiative.org. Standard hydrographic data were collected at the same sites from a rosette fitted with 12 5-liter bottles and a SeaBird 911 CTD containing a SBE-55 temperature sensor, SBE-3 conductivity sensor, SBE45 pressure sensor, and SBE43 oxygen sensor. Additional sensors on the rosette package included a Chelsea Instruments Aqua3 fluorometer and a Biosperical/Licor PAR sensor. Discrete samples were

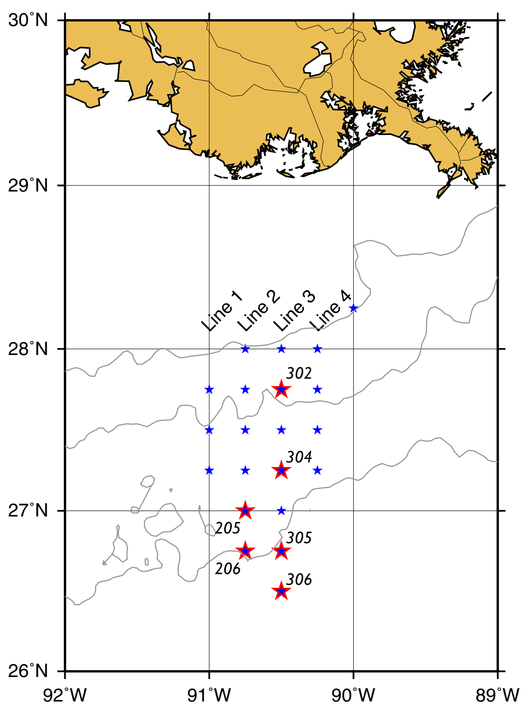

Figure 1 Station positions during cruise PE1521. ^{14}C samples were taken at stations along lines 2 and 3 (larger stars) as shown in Table 2.

https://doi.org/10.1017/RDC.2017.80 Published online by Cambridge University Press

collected from the water bottles for salinity determinations ashore and for oxygen calibration by Winkler titration on board ship. Nutrient samples were collected, filtered, frozen on board and analyzed ashore for nitrate, nitrite, phosphate, silicate, ammonia and urea by standard autoanalyzer methods (WHPO 1994). All data are available from the GRIIDC data repository at https://data.gulfresearchinitiative.org. Note that because the nutrient samples were frozen, the replication in the deep water is not as good as that obtained for temperature, salinity or oxygen, but our shore-based data are very similar to previous data from the deep Gulf of Mexico published by Morrison and Nowlin (1977) and Jochens and DiMarco (2008) and do not suggest any benthic nutrient supply from the slope. Both these authors showed nitrate and silicate maxima at the 800–1000 m depth level within the Antarctic Intermediate Water, with concentrations decreasing below this depth to ~22–24 µmol/L for nitrate and 24–27 µmol/L for silicate, as found on this cruise.

^{14}C samples (500 mL) were collected in pre-combusted glass bottles supplied by the National Ocean Sciences Accelerator Mass Spectrometry facility at Woods Hole, MA (NOSAMS) using established protocols, poisoned with mercuric chloride, and analyzed at NOSAMS. The reproducibility of the method is about 4‰ (Elder et al. 1998). NOSAMS reports the data to two decimal places, but given the reproducibility we report data only to one decimal place. Alkalinity samples were also collected in pre-combusted glass bottles, poisoned with $HgCl_2$ and analyzed ashore using an open-cell auto-titrating method, calibrated daily with buffer solutions and certified reference material seawater samples from Scripps Institution of Oceanography (Dickson 1981; Dickson et al. 2003).

RESULTS

Table 2 shows the measured $\Delta^{14}C$ and $\delta^{13}C$ values, and the estimated apparent ages, as calculated by NOSAMS. NOSAMS uses the methodology of Stuiver and Polach (1977) and Stuiver (1980); see http://www.whoi.edu/nosams/radiocarbon-data-calculations for details of their analytical procedures and corrections. “Modern” in Table 1 means that sample activity is greater than 95% of the ^{14}C activity for AD 1950, as defined by the NBS oxalic acid standard, and that apparent ages are therefore less than 65 yr old. Other ages in this column are relative to 1950.

A vertical plot of $\Delta^{14}C$ against depth is shown in Figure 2a. The $\Delta^{14}C$ in the upper water column varies between 20 and 60‰. Below about 400 m the data describe a smooth curve with a minimum of –100‰ near 1100 m. Below 1150 m the values cluster around –94.6‰ with standard deviation of 3.2‰ (n = 15). If all samples below 900 m are included (n = 20), the mean $\Delta^{14}C$ is –95.4‰, with a standard deviation of 3.4‰, and even considering data below 750 m the mean increases only to –93.6‰. [Note that we are not including the data from Matthews et al. (1973) or Morrison et al. (1983) in these statistics.] On constant density surfaces (Figure 2b), however, the surface inconsistencies largely disappear, with maximum values of 55–65‰ occurring at σ_θ values between 26.4 and 27.0. This is just above the density level of Tropical Atlantic Central Water (27.15; Morrison et al. 1983), which makes up much of the water column above the Florida Strait sill depth.

Figure 2c shows the apparent age of the samples as a function of depth. As expected, the apparent age shows the inverse of $\Delta^{14}C$, with modern ages down to about 500 m depth, which occurs at a σ_θ value of 27.1. The oldest water, at about 1000 m depth, had an apparent age of 800 yr, and below this depth the apparent age decreased to about 730–740 yr.

As a check on sampling reproducibility, three pairs of duplicate samples were taken from station 307, at depths of 1000, 2000, and 2789 m; the differences between the members of each

Table 2 Station positions and ^{14}C data obtained during the cruise.

Stn #	Lat	Long	Date	Depth (m)	$\Delta\ ^{14}C$ ‰	$\delta\ ^{13}C$ ‰	DIC conc. (mmol/kg)	Apparent age (yr)	Age error
302	27°45.32N	90°29.82W	14.4.2015	6	26.6	1.04	1.96	>Modern	
	27°45.32N	90°29.82W		41	37.3	1.01	1.97	>Modern	
	27°45.32N	90°29.82W		84	43.3	0.94	1.98	>Modern	
	27°45.32N	90°29.82W		242	54.2	0.84	2.01	>Modern	
	27°45.32N	90°29.82W		324	33.0	0.58	2.11	>Modern	
	27°45.32N	90°29.82W		402	10.1	0.61	2.12	>Modern	
	27°45.32N	90°29.82W		482	–29.3	0.63	2.13	175	20
	27°45.32N	90°29.82W		558	–39.8	0.71	2.14	265	20
	27°45.32N	90°29.82W		639	–56.7	0.69	2.16	405	15
	27°45.32N	90°29.82W		718	–74.1	0.80	2.15	555	15
	27°45.32N	90°29.82W		800	–83.7	0.81	2.15	640	15
304	27°14.46N	90°30.02W	15.4.2015	6	45.5	1.06	1.98	>Modern	
	27°14.46N	90°30.02W		49	59.0	0.61	2.09	>Modern	
	27°14.46N	90°30.02W		150	28.4	0.61	2.11	>Modern	
	27°14.46N	90°30.02W		300	61.3	0.61	2.10	>Modern	
	27°14.46N	90°30.02W		400	–5.8	0.66	2.13	>Modern	
	27°14.46N	90°30.02W		500	–38.7	0.68	2.15	255	15
	27°14.46N	90°30.02W		600	–67.8	0.73	2.15	500	25
	27°14.46N	90°30.02W		698	–89.9	0.82	2.14	695	15
	27°14.46N	90°30.02W		900	–97.7	0.91	2.16	760	15
	27°14.46N	90°30.02W		1100	–102.2	0.94	2.16	805	15
	27°14.46N	90°30.02W		1248	–97.3	1.04	2.13	760	15
306	26°45.01N	90°30.04W	17.4.2015	100	65.1	0.67	2.10	>Modern	
	26°45.01N	90°30.04W		193	62.3	0.59	2.13	>Modern	
	26°45.01N	90°30.04W		401	2.6	0.59	2.16	>Modern	
	26°45.01N	90°30.04W		599	–48.3	0.67	2.16	335	15
	26°45.01N	90°30.04W		797	–88.5	0.80	2.15	680	15
	26°45.01N	90°30.04W		987	–99.7	0.91	2.15	780	20
	26°45.01N	90°30.04W		1154	–101.2	0.92	2.15	795	15
	26°45.01N	90°30.04W		1902	–90.9	0.98	2.15	705	20

Table 2 (*Continued*)

Stn #	Lat	Long	Date	Depth (m)	Δ ^{14}C ‰	δ ^{13}C ‰	DIC conc. (mmol/kg)	Apparent age (yr)	Age error
	26°45.01N	90°30.04W		2202	–95.8	0.97	2.14	745	15
	26°45.01N	90°30.04W		2469	–94.3	0.95	2.14	735	25
307	26°28.93N	90°28.04W	17.4.2015	202	54.8	0.52	2.12	>Modern	
	26°28.93N	90°28.04W		399	3.0	0.56	2.15	>Modern	
	26°28.93N	90°28.04W		597	–58.8	0.72	2.06	425	15
	26°28.93N	90°28.04W		800	–83.7	0.79	2.15	640	25
	26°28.93N	90°28.04W		1001	–95.9	0.79	2.16	745	25
	26°28.93N	90°28.04W		1001	–92.8	0.84	2.16	720	15
	26°28.93N	90°28.04W		1301	–90.4	0.95	2.15	700	15
	26°28.93N	90°28.04W		1600	–92.5	0.98	2.14	715	20
	26°28.93N	90°28.04W		2002	–94.6	1.02	2.15	735	15
	26°28.93N	90°28.04W		2002	–92.3	0.98	2.16	715	15
	26°28.93N	90°28.04W		2402	–93.9	0.98	2.15	730	15
	26°28.93N	90°28.04W		2788	–95.1	1.01	2.16	740	15
	26°28.93N	90°28.04W		2788	–94.5	1.01	2.14	735	20
205	26°45.11N	90°45.12W	17.4.2015	1830	–90.2	0.97	2.14	695	15
206	26°59.99N	90°45.01W	17.4.2015	1401	–98.6	0.97	2.13	770	15
	26°59.99N	90°45.01W		1621	–97.8	0.96	2.13	765	15

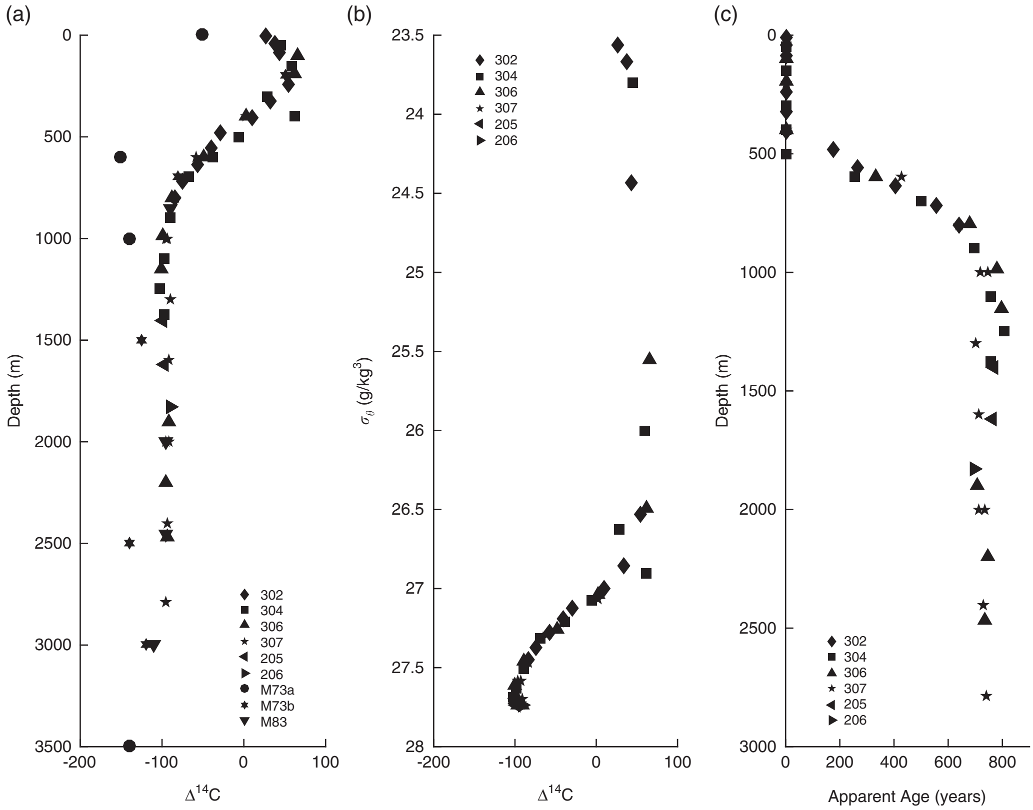

Figure 2 $\Delta^{14}C$ concentrations as a function of (a) depth and (b) density, and apparent age as a function of depth (c). M73a, M73b and M83 in (a) refer to early data from Matthews et al. (1973) and Morrison et al. (1983); see text for details.

pair were 3.1, 2.3, and 0.6‰ respectively, which is considerably less than the error estimates from NOSAMS (±4‰).

DISCUSSION

Based on data collected during the GEOSECS program in the 1970s, the replacement times for the deep waters of the world's oceans were estimated to be 275, 250, and 550 yr, respectively, for the Atlantic, Indian, and Pacific Oceans (Stuiver et al. 1983). However, these estimates do not necessarily coincide with the apparent regional age of the water calculated from $\Delta^{14}C$ changes. Matsumoto and Key (2004), for example, using the large data set collected during the WOCE program in the 1990s (Key et al. 2004), showed that the measured $\Delta^{14}C$ of deep water at 3500 m in the Atlantic varied from about –50‰ in the Labrador Sea to about –160‰ in the Southern Ocean. These have apparent ages of about 400 and 1500 yr respectively, giving an initial offset of 400 yr for North Atlantic surface water. The –50‰ value from the Labrador Sea shows that even the deep water in this region was contaminated with bomb radiocarbon (^{14}C) by this time, and the pre-bomb surface value is thought to be about –60‰ (Östlund and Rooth 1990; Matsumoto and Key 2004). To get a "true" age of deep water one has to consider the difference in $\Delta^{14}C$ between water sinking in the polar North Atlantic (–50‰) and that found around Antarctica (–160‰), as was pointed out initially by Broecker (1979). A good discussion of how to correct for mixing of different water masses is given by Matsumoto (2007).

https://doi.org/10.1017/RDC.2017.80 Published online by Cambridge University Press

Three deep stations in the Gulf of Mexico have been sampled previously for $\Delta^{14}C$, at 24°30′N, 94°00′W in 1962 and at 23°45′N, 92°38′W in 1971 (Matthews et al. 1973), and at 23°01′N, 92°28′W in 1978 by Morrison et al. (1983). Those samples, which all came from the southwestern GoM, were all obtained using the large-volume sampling method (~250-L samples) combined with β-decay counting rather than the small-volume-AMS methodology used here. The data, shown in Figure 2a, were however inconsistent and implied that bomb-produced ^{14}C in the deep western Gulf of Mexico had increased down to 3000 m during the seven years between the last two cruises, with $\Delta^{14}C$ increasing from –140‰ to about –90‰. This did not agree with tritium data, which showed no penetration below about 700 m. Morrison et al. (1983) therefore concluded that the earlier data were inaccurate. The $\Delta^{14}C$ data reported by Morrison had an estimated uncertainty of ± 4‰, but their deep water values ranged between –80‰ and –100‰, with a minimum near 3000 m. One possible cause of the unexpected noise in these samples was the fact that the large volume samples had to be collected using repeated casts with 30-L Niskin bottles rather than the more conventional 250-L Gerard barrels commonly used at that time.

Based on GEOSECS data, the pre-bomb surface ocean $\Delta^{14}C$ value is thought to have been about –60‰ (Östlund and Rooth 1990; Matsumoto and Key 2004), although Broecker (1979) used –69‰. Deep water values are lower (more negative) owing to radioactive decay during circulation within the thermohaline (Druffel 2002; Toggweiler and Key 2002; Key et al. 2004). During the late 1950s and especially the first half of the 1960s, atmospheric testing of thermonuclear weapons caused a huge increase in the atmospheric $\Delta^{14}C$ (Hua et al. 2013), leading to more positive values for $\Delta^{14}C$, and this added ^{14}C has been slowly working its way deeper into the water column. Once atmospheric bomb-testing ceased, the atmospheric $\Delta^{14}C$ level rapidly decreased as the atmospheric ^{14}C was deposited, primarily as $^{14}CO_2$, onto land and into the surface ocean. The net atmosphere-ocean flux of ^{14}C is now near zero and in some places there is a flux from the ocean back to the atmosphere (Graven et al. 2012). The –60‰ value, equivalent to the earlier surface or present day deep Labrador Sea concentrations, is now found at about 600–650 m, well above the Florida Strait sill depth of ~740 m.

Local increases of $\Delta^{14}C$ to more positive values reflect the downward movement of bomb-produced ^{14}C in the source waters of the Loop Current in both the North and South Atlantic, while constant values of about –95‰ are achieved at about 900 m depth. Antarctic Intermediate Water, which might also be expected to show an increase in $\Delta^{14}C$ because of its formation near the surface in the southern hemisphere with $\Delta^{14}C$ somewhere near –110‰ (Matsumoto and Key 2004), is characterized by a salinity minimum and found at or about the depth of the Florida Strait sill (Rivas et al. 2005; Table 1), and our data suggest a value of about –85‰ here (Table 2). This is in reasonable agreement with measurements in the western Atlantic of ~–80‰ (Ostlund and Rooth 1990). A minimum in $\Delta^{14}C$ slightly below this depth coincides with the oldest apparent age (Figure 2c); a similar feature was also found in samples from around 1000 m depth in the subtropical and tropical North Atlantic by Östlund et al. (1974) and may denote homogeneous mixing of abyssal waters of slightly younger age within the Caribbean Sea. At the time of sampling, the Loop Current extended well into the northern Gulf with its western boundary between 90° and 91°W and its northern boundary near 28°N, as shown by altimetric sea surface height measurements (Figure 3), and the influence of this current is known to extend from the surface to below 1200 m depth. Therefore, it is likely that we sampled a mixture of GoM and Caribbean water in this depth range.

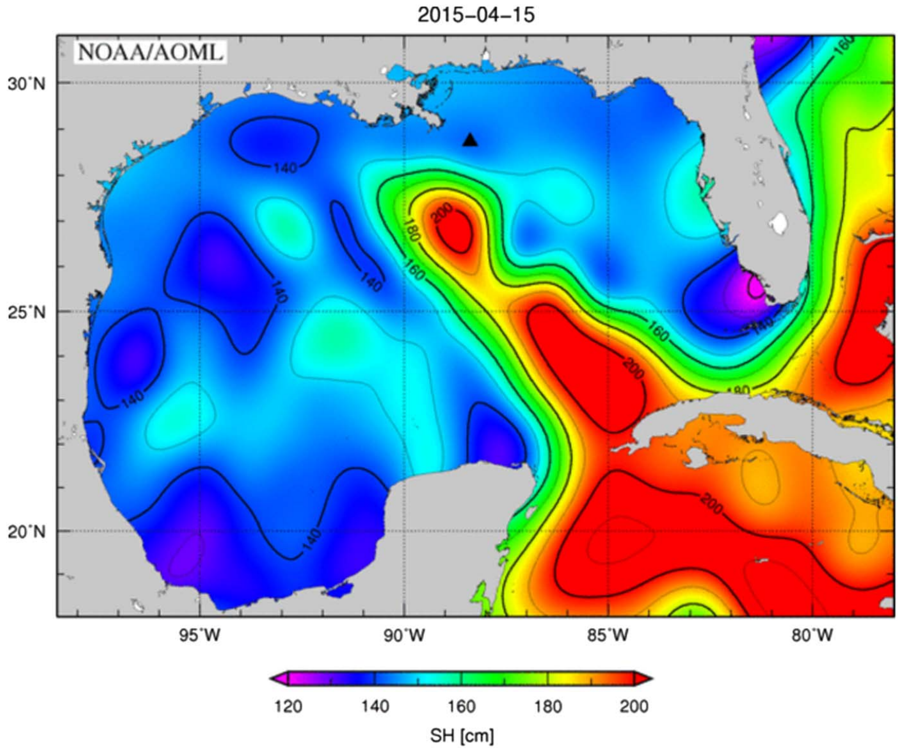

Figure 3 Sea surface height in the Gulf of Mexico for 15 April 2015. Image from http://www.aoml.noaa.gov/phod/dhos/altimetry.php.

As a check on our data, we have estimated the "natural" Δ^{14}C values from the relationships between "natural" Δ^{14}C with silica (Broecker et al. 1995) and total alkalinity (Rubin and Key 2002; Table 3). This is required to take account of the decomposition of any particulate carbon (mostly diatoms) that would otherwise interfere in the estimation of the ^{14}C:^{12}C ratio by making it more positive through the incorporation of additional sea surface carbon. For the silica method

$$\text{“Natural”}\Delta^{14}\text{C} = -70 - [\text{Si}] \quad (1)$$

where –70 is the theoretical surface value obtained from models (Graven et al. 2012) and [Si] is the silicate concentration in μmol/kg (Broecker et al. 1995). These calculations give numbers in excellent agreement with the measured values; for 24 samples taken at depths of 750 m or below, the mean "natural" Δ^{14}C value is –94.9‰, with standard deviation of 2.3‰, again well within the 4‰ error of the measurements. Thus, the mean apparent age of the deep water in the Gulf of Mexico below 900 m is about 740 ± 32 yr. Using the slightly different Δ^{14}C–Si relationship of Rubin and Key (2002) for the Atlantic

$$\text{Natural}\,\Delta^{14}\text{C} = -82 - 0.68[\text{Si}] \quad (2)$$

the mean value for natural Δ^{14}C deeper than 800 m is –99.1 with standard deviation 1.1‰.

The potential alkalinity method relies on the relationship between ^{14}C and alkalinity when the latter has been corrected for biological activity (Rubin and Key 2002). This is then normalized to a salinity of 35 via Equation (3) (Brewer and Goldman 1976) and "natural" Δ^{14}C is calculated from Equations (4) or (5), depending on whether one uses the global Equation (4) or that

https://doi.org/10.1017/RDC.2017.80 Published online by Cambridge University Press

Table 3 Chemical data for determining the "natural" $\Delta^{14}C$ values (to nearest 0.1‰) based on their relationships with silicate (a) or alkalinity (b, c). Alkalinity calculations use either the general relationship for the global oceans (b) or that for the Atlantic (c) developed by Rubin and Key (2002). See text for details. All $\Delta^{14}C$ values are in ‰.

Stn #	Depth (m)	Salinity	Si (μmol/kg)	Natural $\Delta^{14}C$ (a)	NO_3 (μmol/kg)	Alkalinity (μmol/kg)	Natural $\Delta^{14}C$ global (b)	Natural $\Delta^{14}C$ Atlantic (c)
302	6	36.169	0.00	–70.00	0.00	2303.29	28.70	37.57
	41	36.233	0.00	–70.00	0.00	2301.98	33.71	42.77
	84	36.490	0.00	–70.00	0.31	2376.80	–20.59	–13.68
	242	36.288	0.00	–70.00	1.39	2384.10	–40.56	–34.43
	324	35.673	4.79	–74.79	18.58	2345.58	–58.60	–53.18
	402	35.367	9.34	–79.34	25.10	2342.25	–80.89	–76.36
	482	35.109	10.70	–80.70	22.18	2252.46	–8.54	–1.15
	558	35.003	12.86	–82.86	23.35			
	639	34.934	17.27	–87.27	28.93	2275.17	–47.91	–42.07
	718	34.880	16.43	–86.43	23.33	2315.48	–84.83	–80.45
	800	34.896	20.79	–90.79	25.90	2262.76	–35.45	–29.12
304	6	36.259	0.00	–70.00	9.97			
	49	36.671	0.97	–70.97	5.97	2380.25	–18.10	–11.09
	150	36.112	3.11	–73.11	12.75	2404.21	–80.70	–76.16
	300	35.567	8.13	–78.13	21.51	2375.11	–95.97	–92.03
	400	35.172	12.59	–82.59	26.66	2291.33	–46.19	–40.28
	500	34.996	17.84	–87.84	30.16	2281.11	–50.84	–45.12
	600	34.912	20.89	–90.89	31.28	2306.88	–82.12	–77.63
	698	34.904	24.25	–94.25	32.66	2318.98	–95.66	–91.70
	900	34.930	25.06	–95.06	26.51	2276.33	–46.90	–41.03
	1100	34.950	24.25	–94.25	24.14	2314.73	–80.39	–75.84
	1248	34.962	24.25	–94.25	23.08	2293.33	–57.95	–52.51
306	100	36.757	1.42	–71.42	4.57	2406.71	–35.93	–29.61
	193	36.309	3.17	–73.17	10.67	2375.20	–39.60	–33.43
	401	35.276	12.18	–82.18	23.86	2324.23	–68.37	–63.34
	599	34.945	19.50	–89.50	28.71	2315.53	–85.89	–81.55
	797	34.899	24.68	–94.68	29.82	2324.38	–98.46	–94.61
	987	34.926	26.58	–96.58	26.75	2343.28	–111.98	–108.67
	1154	34.943	26.75	–96.75	24.71	2335.68	–101.53	–97.81
	1902	34.966	25.63	–95.63	22.77	2334.66	–97.25	–93.36
	2202	34.967	28.04	–98.04	22.30	2344.26	–105.91	–102.36
	2469	34.968	27.36	–97.36	22.65	2346.42	–108.32	–104.87
307	202	36.084	4.15	–74.15	13.40			
	399	35.232	13.33	–83.33	25.71	2372.38	–118.91	–115.87
	597	34.922	21.13	–91.13	30.82	2319.27	–93.01	–88.95
	800	34.900	24.92	–94.92	29.78	2310.19	–84.64	–80.26
	1001	34.920	26.10	–96.10	27.68	2332.29	–102.63	–98.95
	1001	34.920	26.10	–96.10	27.68	2332.29	–102.63	–98.95
	1301	34.951	26.17	–96.17	24.30	2332.36	–97.42	–93.53
	1600	34.960	24.99	–94.99	22.05	2347.33	–109.09	–105.67
	2002	34.964	25.51	–95.51	22.83	2348.94	–111.15	–107.81
	2002	34.964	25.51	–95.51	22.83	2330.37	–93.27	–89.22
	2402	34.966	25.20	–95.20	23.02	2348.94	–111.17	–107.84

https://doi.org/10.1017/RDC.2017.80 Published online by Cambridge University Press

Table 3 (*Continued*)

Stn #	Depth (m)	Salinity	Si (µmol/kg)	Natural $\Delta^{14}C$ (a)	NO_3 (µmol/kg)	Alkalinity (µmol/kg)	Natural $\Delta^{14}C$ global (b)	Natural $\Delta^{14}C$ Atlantic (c)
	2788	34.968	24.99	–94.99	22.23	2339.73	–101.45	–97.73
	2788	34.968	24.99	–94.99	22.23	2339.73	–101.45	–97.73
205	1830	34.965	22.27	–92.27	18.57			
206	1401	34.962	26.71	–96.71	22.31	2327.90	–90.53	–86.38
	1621	34.965	23.21	–93.21	19.38	2362.94	–121.24	–118.30

based on Atlantic data, Equation (5). The difference between the two is 3–4‰, with the Atlantic equation giving more positive values.

$$\text{Palk} = (\text{alkalinity} + \text{nitrate}) \times 35/\text{salinity} \tag{3}$$

$$\text{Natural } \Delta^{14}C = -59.0 - 0.962 \times (\text{Palk} - 2320) \tag{4}$$

$$\text{Natural } \Delta^{14}C = -53.6 - 1.000 \times (\text{Palk} - 2320) \tag{5}$$

Using Equations (3) and (4) gives slightly lower natural $\Delta^{14}C$ values of –100.4‰ (standard deviation 10.7‰) for samples below 750 m depth decreasing to -104.0 ± 8.8‰ if only samples from below 1150 m are considered, but this is still within any likely error. Use of Equation (5) gives ranges of -96.6 ± 11.1‰ for samples below 750 m and -100.4 ± 9.1‰ if only those from deeper than 1150 m are considered. The modification to the potential alkalinity method proposed by Sweeney et al. (2007), primarily for lower thermocline Pacific waters, has negligible impact on the deep GoM samples due to the relatively high oxygen concentrations.

It is perhaps not surprising that there is little difference between the measured $\Delta^{14}C$ values and the "natural" values (see Table 3) estimated by Equations (1–5). This is because the deep GoM is known to be oligotrophic, so very little particulate carbon is likely to reach the deep waters except over the upper slope, where particulate organic carbon concentrations are typically 1–3 µmol/L (Cherrier et al. 2014; W Gardner, personal communication) and advection of material from the shelf may occur, although we did not see this during the cruise. However, it is possible that recent bomb carbon has been transported into the deep GoM through sinking organic matter produced at the surface. Cherrier et al. (2014) found that in De Soto canyon, east of the Mississippi delta, following the Deepwater Horizon rig blowout, particulate matter showed highly depleted $\Delta^{14}C$ and $\delta^{13}C$ values at depth and a positive relationship between them. This was attributed to surface organisms ingesting depleted oil and gas residues following the spill. A plot of $\Delta^{14}C$ against $\delta^{13}C$ for our samples shows a negative slope, with $\delta^{13}C$ increasing through the thermocline as $\Delta^{14}C$ decreases, and roughly constant values of 0.95–1.04 for all samples from below 1000 m depth. This could therefore be attributed to bomb carbon being transported into the deep GoM, and would mean that our estimated age of the deep water is a minimum.

The only entrance to the GoM is via Yucatan Strait from the Caribbean, which in turn contains a well-mixed deep water mass. Although many passages connect the Caribbean Sea to the Atlantic Ocean, the deepest channel, the Anegada-Jungfern Passage between Puerto Rico and

St Croix, has a sill depth of only 1815 m at its western end in the Jungfern Passage at 17°35.1′N, 65°14.2′W (Fratantoni et al. 1997). Thus, it is unnecessary to consider any water mass below the upper NADW in terms of a source for deep water in the Caribbean and GoM. There are only three records of ^{14}C data from the eastern Caribbean; one set was taken in the Venezuela Basin in 1973 (Ribbat et al. 1976) and gave a mean $\Delta^{14}C$ of –89.3‰ for all depths below 1500 m. Broecker et al. (1991) point out that the ^{14}C decay rate is equivalent to a loss of 10‰ in 80 yr, so assuming no deeper penetration of bomb carbon in the region, these data are equivalent to a present day concentration of about –94.3‰, in good agreement with our data from the Gulf. More recently, a station was occupied at 66°W, 14.35°N during the occupation of WOCE line A22 in 1997 (Johnson et al. 2003). The mean natural ^{14}C value below 1500 m was about –108 ± 8‰, calculated according to Sweeney et al. (2007), suggesting very slow replenishment of the deep water in the 4500-m-deep basin. However, the data seem to show invasion by bomb ^{14}C between 1500 and 2800 m depth, as is also clearly shown by tritium data from this cruise. More recent CLIVAR data taken along the same A22 line during 2012 suggest little or no pre-bomb carbon below about 800 m depth ($\Delta^{14}C$ ~–90‰), but there are only very limited data from below 2000 m (R M Key, personal communication). Tritium, however, is observable throughout the water column in this basin. As discussed above, this suggests that ^{14}C has invaded the deep Caribbean and again means that our estimates for the age of the deep water may be too young. Further samples from this region are needed to clarify this.

Despite the well-mixed nature of the deep water in the GoM, a section along approximately 90°30′W shows some apparent structure in both density and $\Delta^{14}C$ (Figure 4). Water between about 900 and 1400 m at stations 304 and 306 had the lowest $\Delta^{14}C$ concentrations at about –100‰ and appears to be somewhat older than the rest of the water sampled, while the water immediately below it seems to be somewhat denser (σ_θ >27.73) than elsewhere. Östlund et al. (1974) and Östlund and Rooth (1990) showed a minimum in $\Delta^{14}C$ of the same magnitude at this depth at 21°N in their analysis of ^{14}C data from the Atlantic GEOSECS and TTO cruises, and it is tempting to suggest that the values seen here result from the advection of this water mass into the Gulf of Mexico in the Loop Current via the Caribbean (see Figure 3). It is unclear where this minimum comes from, although it is also seen as a local minimum or inflection in tritium data from the same stations in the subtropical Atlantic (Östlund et al. 1974). It seems too deep to be Antarctic Intermediate Water, which is found at a depth of about 750 m in the western subtropical North Atlantic and has a $\Delta^{14}C$ of –80 to –85‰, and does not coincide with any particular parameter inflection according to WOCE data (Koltermann et al. 2011). However, allowing for radioactive decay since the GEOSECS data (1972) and TTO data (1981) were collected, and the fact that Östlund et al. (1974) did not correct their data for potential interference from biology, one would expect $\Delta^{14}C$ to be nearer –105‰ than the –100‰ we observed. Water at this depth can, of course, enter the Caribbean further north than the deeper water, through the Windward Passage between Cuba and Hispaniola, and as the ^{14}C signal has presumably penetrated further into the water column since the TTO transects this would make the $\Delta^{14}C$ value more positive and possibly cancel out the expected decay.

An alternative possibility is that the water on the slope of the northern Gulf of Mexico has been contaminated by "dead" carbon. Hundreds of active seeps are known on the shelf and slope in this region (MacDonald et al. 1993, 1996, 2002) and because the oil formations were laid down millions of years ago, any carbon released by them will be radiologically "dead." This will affect the ^{14}C:^{12}C ratio used to calculate the $\Delta^{14}C$ value, pushing it towards more negative values. Our samples were taken across the slope in an area where active drilling for oil and gas is occurring,

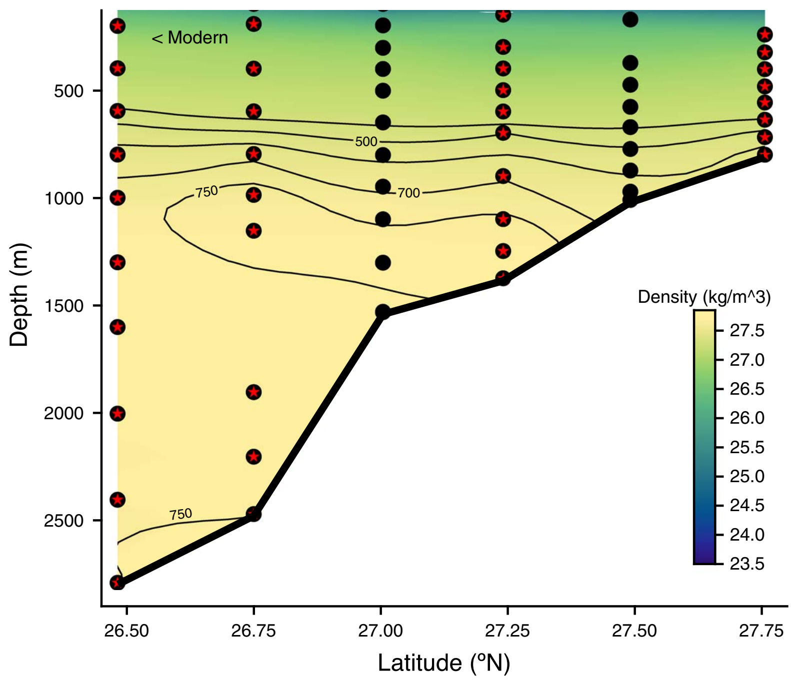

Figure 4 Apparent age as a function of depth and density for the ^{14}C samples taken along 90°30′W. Discrete samples are shown by circles, with red circles showing the ^{14}C sampling sites. Contour lines show the apparent age in years.

and Figure 4 shows that the oldest apparent ages were found adjacent to the slope between about 850 and 1200 m depth. Although background levels of dissolved oil are generally very low (Wade et al. 2016), many of the wells also contain high gas concentrations, and the oxidation of dissolved gas leaking from these seeps may be able to affect the ratio and thus the apparent age. However, the lack of any obvious variability in $\delta^{13}C$ values below 1000 m depth (see Table 2) suggests that any such contamination is minimal.

As stated above, the apparent age based on $\Delta^{14}C$ is not the actual age of the water sample. This may be calculated, however, by making the necessary corrections, as per Matsumoto (2007). Because deep water in the Atlantic Ocean is a mixture of water from the Arctic and Antarctic, one has first to determine how much each source contributes to a particular water sample. Broecker et al. (1991) showed that NADW at 2400 m depth contained more than 90% northern water. As the deepest water that feeds the Caribbean is from 500 m shallower than this, we can probably ignore any contribution from the Antarctic other than a small contribution from AAIW and assume that all the water comes originally from the northern North Atlantic. Broecker et al. (1991) in fact state that the effect of AAIW is likely important only south of about 30°S, so we have ignored its possible influence. However, one still has to reset the reservoir age of the northern deep water to zero so that the measured age is then the time elapsed since the water parcel was isolated from the atmosphere. For northern source water this is done by subtracting –67‰ from the measured $\Delta^{14}C$ concentration; for any Antarctic component the correction is –140‰ (Broecker et al. 1998). These corrections need to be weighted by the percentage of each water source in the sample, which in this case is 1.0 as we are only considering a northern source.

The new residual $\Delta^{14}C$ value is converted to a "circulation age" by application of Equation (6)

$$A = -8033 \times \ln\left(1 + \Delta^{14}C/1000\right) \quad (6)$$

where A is the circulation age and $\Delta^{14}C$ is the depth averaged residual. Taking the mean measured value for our samples below 900 m depth of –95.4 ± 3.4‰, this gives a circulation age for the water in the deep Gulf of Mexico of 231 ± 28 yr. If, instead, we use the natural $\Delta^{14}C$ age determined using Equations (3) and (4), then the circulation age becomes 293 ± 74 yr. Using the Atlantic Equation (5) produces an intermediate age of about 263 ± 84 yr. All these estimates are in good agreement with the heat flux estimate of Rivas et al (2005), as well as a basic calculation of residence time for the deep water by Matthews et al. (1973) of 270 yr. These ages also put upper limits on the age of the deep water in the Caribbean Sea, given that this is the source of deep water in the Gulf of Mexico, and agree with the original estimate of a 275-yr turnover time for the deep Atlantic by Stuiver et al. (1983). If anything, because of the caveats considered above, particularly the potential for invasion of the Caribbbean and GoM by bomb carbon, these will be minimum ages. However, additional measurements from other parts of the regional seas, coupled with tracers such as tritium or CFCs, are needed to confirm this and provide additional data on the penetration of anthropogenic gases into the Gulf of Mexico and the Caribbean.

ACKNOWLEDGMENTS

We thank the captain and crew of the *R. V. Pelican* for their seamanship during the cruise. This research was made possible by a grant to the Gulf Integrated Spill Consortium from the Gulf of Mexico Research Initiative. Data are archived at and are publically available from the Gulf of Mexico Research Initiative Information and Data Cooperative (GRIIDC) at https://data.gulfresearchinitiative.org as data sets R1.x137.000:0004 (doi:10.7266/N7Z60M3Z) and R1.x137.131:0006 (doi:10.7266/N7M32ST2). NOSAMS is supported by NSF through Cooperative Agreement OCE-1239667.

REFERENCES

Alvera-Azcarate A, Barth A, Weisberg RH. 2009. The surface circulation of the Caribbean Sea and the Gulf of Mexico as inferred from satellite altimetry. *Journal of Physical Oceanography* 39:640–57.

Badan A, Candela J, Sheinbaum J, Ochoa J. 2005. Upper-layer circulation in the approaches to Yucatan Channel. In: Sturges W, Lugo-Fernandez A, editors. *Circulation in the Gulf of Mexico: Observations and Models. Geophysical Monographs* 161. American Geophysical Union. p 57–69.

Brewer PG, Goldman JC. 1976. Alkalinity changes generated by phytoplankton growth. *Limnology and Oceanography* 21:108–17.

Broecker WS. 1979. A revised estimate for the radiocarbon age of North Atlantic Deep Water. *Journal of Geophysical Research* 84:3218–26.

Broecker WS, Blanton S, Smethie WM Jr. 1991. Radiocarbon decay and oxygen utilization in the deep Atlantic Ocean. *Global Biogeochemical Cycles* 5:87–117.

Broecker WS, Sutherland S, Smethie W, Peng T-H, Östlund G. 1995. Oceanic radiocarbon: separation of the natural and bomb components. *Global Biogeochemical Cycles* 9:263–88.

Broecker WS, Peacock SL, Walker S, Weiss R, Fahrbach E, Schroeder M, Mikolajewic U, Heinze C, Key R, Peng T-H, Rubin S. 1998. How much deep water is formed in the Southern Ocean? *Journal of Geophysical Research* 103:15,833–44.

Bunge L, Ochoa J, Badan A, Candela J, Sheinbaum J. 2002. Deep flows in the Yucatan channel and their relation to changes in the Loop Current extension. *Journal of Geophysical Research* 107:3233. DOI: 10.1029/2001JC001256.

Candela J, Tanahara S, Crepon M, Barnier B, Sheinbaum J. 2003. Yucatan Channel flow: observations versus CLIPPER ATL6 and MERCATOR PAM models. *Journal of Geophysical Research* 108:3385. DOI: 10.1029/2003JC001961.

Cherrier J, Sarkodee-Adoo J, Guilderson TP, Chanton JP. 2014. Fossil carbon inmparticulate organic matter in the Gulf of Mexico following the Deepwater Horizon event. *Environmental Science and Technology Letters* 1:108–12.

Cherubin LM, Sturges W, Chassignet EP. 2005. Deep flow variability in the vicinity of the Yucatan Straits from a high-resolution numerical simulation. *Journal of Geophysical Research* 110: C04009. DOI: 10.1029/2004JC002280.

DeHann CJ, Sturges W. 2005. Deep cyclonic circulation in the Gulf of Mexico. *Journal of Physical Oceanography* 35:1801–12.

Dickson AG. 1981. An exact definition of total alkalinity and a procedure for the estimation of alkalinity and total inorganic carbon from titration data. *Deep-Sea Research* 28A:609–23.

Dickson AG, Afghan JD, Anderson GC. 2003. Reference materials for oceanic CO_2 analysis: a method for the certification of total alkalinity. *Marine Chemistry* 80:185–97.

Druffel ERM. 2002. Radiocarbon in corals: records of the carbon cycle, surface circulation and climate. *Oceanography* 15(1):122–7. DOI: 10.5670/oceanog.2002.43.

Elder KL, McNichol A, Gagnon AR. 1998. Reproducibility of seawater, inorganic carbon ^{14}C results at NOSAMS. *Radiocarbon* 40(1):223–30.

Fratantoni DM, Zantopp RJ, Johns WE, Miller JL. 1997. Updated bathymetry of the Anagada-Jungfern Passage complex and implications for Atlantic inflow to the abyssal Caribbean Sea. *Journal of Marine Research* 55:847–60.

Graven HD, Gruber N, Key R, Khatiwala S, Giraud X. 2012. Changing controls on oceanic radiocarbon:New insights on shallow-to-deep ocean exchange and anthopogenic CO_2 uptake. *Journal of Geophysical Research* 117:C10005. DOI: 10.1029/2012JC008074.

Hamilton P. 1990. Deep currents in the Gulf of Mexico. *Journal of Physical Oceanography* 20:1087–104.

Hamilton P, Singer JJ, Waddell E, Donohue K. 2003. *Deepwater observations in the northern Gulf of Mexico from in-situ current meters and PIES*. OCS Study MMS 2003-049, Final Report to U.S. Minerals Management Service, Vol. 2, Gulf of Mexico OCS Region. 95 p.

Hamilton P, Bower A, Furey H, Leben R, Perez-Brunius P. 2016. *Deep Circulation in the Gulf of Mexico: A Lagrangian Study*. U.S. Dept. of the Interior, Bureau of Ocean Energy Management, Gulf of Mexico OCS Region, New Orleans, LA. OCS Study BOEM 2016-081. 289 p.

Hua Q, Barbetti M, Rakowski AZ. 2013. Atmospheric radiocarbon for the period 1950–2010. *Radiocarbon* 55(4):2059–72.

Jochens AE, DiMarco SF. 2008. Physical oceanographic conditions in the deepwater Gulf of Mexico in summer 2000–2002. *Deep-Sea Research II* 55:2541–54.

Jochens AE, Bender LC, DiMarco SF, Morse JW, Kennicutt MC II, Howard MK, Nowlin WD Jr. 2005. *Understanding the Processes that Maintain the Oxygen Levels in the Deep Gulf of Mexico: Synthesis Report*. U.S. Dept. of the Interior, Minerals Management Service, Gulf of Mexico OCS Region, New Orleans, LA. OCS Study MMS 2005-032. 142 p.

Johns WE, Townsend TL, Fratantoni DM, Wilson WD. 2002. On the Atlantic inflow to the Caribbean Sea. *Deep-Sea Research I* 49:211–43.

Johnson K, Key R, Millero F, Sabine C, Wallace D, Winn C, Arlen L, Erickson K, Friis K, Galanter M, Goen J, Rotter R, Thomas C, Wilke R, Takahashi T, Sutherland S. 2003. Carbon Dioxide, Hydrographic, and Chemical Data Obtained During the R/V Knorr Cruises in the North Atlantic Ocean on WOCE Sections AR24 (November 2–December 5, 1996) and A24, A20, and A22 (May 30–September 3, 1997). In: Kozyr A, editor. ORNL/CDIAC-143, NDP-082. Carbon Dioxide Information Analysis Center, Oak Ridge National Laboratory, U.S. Department of Energy, Oak Ridge, Tennessee. DOI: 10.3334/CDIAC/otg.ndp082.

Key RM, Kozyr A, Sabine CL, Lee K, Wanninkhof R, Bullister JL, Feely RA, Millero FJ, Mordy C, Peng T-H. 2004. A global ocean carbon climatology:Results from Global Data Analysis Project (GLODAP). *Global Biogeochemical Cycles* 18: GB4031. DOI: 10.1029/2004GB002247.

Koltermann KP, Gouretski VV, Jancke K. 2011. *Hydrographic Atlas of the World Ocean Circulation Experiment (WOCE). Volume 3: Atlantic Ocean*. Sparrow M, Chapman P, Gould J, editors). International WOCE Project Office, Southampton, UK. ISBN 090417557X.

Ledwell JR, He R, Xue Z, DiMarco SF, Spencer L, Chapman P. 2016. Dispersion of a tracer in the deep northern Gulf of Mexico. *Journal of Geophysical Research* 121:1110–32. DOI: 10.1002/2015JC011405.

MacDonald IR, Guinasso NL Jr, Ackleson G, Amos JF, Duckworth R, Sassen R, Brooks JM. 1993. Natural oil slicks in the Gulf of Mexico visible from space. *Journal of Geophysical Research* 98:16351–64.

MacDonald I, Reilly JF Jr, Best SR, Venkataramaiah R, Sassen R, Amos J, Guinasso NL Jr. 1996. A remote-sensing inventory of active oil seeps and chemosynthetic communities in the northern Gulf of Mexico. In: Schumacher D, Abrams MA, editors. *Hydrocarbon Migration and its Near-Surface Expression*. AAPG Memoir 66:27–37. Tulsa, OK: American Association of Petroleum Geologists.

MacDonald IR, Leifer I, Sassen R, Stine P, Mitchell R, Guinasso N. 2002. Transfer of hydrocarbons from natural seeps to the water column and atmosphere. *Geofluids* 2:95–107.

Matsumoto K. 2007. Radiocarbon-based circulation age of the world oceans. *Journal of Geophysical Research* 112:C09004. DOI: 10.1029/2007JC 004095.

Matsumoto K, Key RM. 2004. Natural radiocarbon distribution in the deep ocean. In: Shiyomi M,

et al., editors. *Global Environmental Change in the Ocean and on Land*. p 45–58.
Matthews TD, Fredericks AD, Sackett WM. 1973. The geochemistry of radiocarbon in the Gulf of Mexico. *Report IAEA-SM-158148*. Vienna: International Atomic Energy Agency. p 725–34.
Maul GA, Mayer DA, Baig SR. 1985. Comparisons between a continuous 3-year current-meter observation at the sill of the Yucatan Strait, measurements of Gulf Loop Current area, and regional sea level. *Journal of Geophysical Research* 90:9089–96.
Molinari RL, Mayer D. 1980. Physical oceanographic conditions at a potential OTEC site in the Gulf of Mexico; 27.5°N, 85.5°W. *NOAA Tech. Memo ERL-AOML-42*. 100 p.
Morrison JM, Nowlin WD Jr. 1977. Repeated nutrient, oxygen and density sections through the Loop Current. *Journal of Marine Research* 35:105–28.
Morrison JM, Merrill WJ, Key RM, Key TC. 1983. Property distributions and deep chemical measurements within the western Gulf of Mexico. *Journal of Geophysical Research* 88:2601–8.
Nowlin WD Jr, McClellan H. 1967. A characterization of the Gulf of Mexico waters in winter. *Journal of Marine Research* 25:29–59.
Nowlin WD Jr, Jochens AE, DiMarco SF, Reid RO, Howard MK. 2001. *Deepwater physical oceanography reanalysis and synthesis of historical data: Synthesis report*. OCS Study MMS 2001-064, U.S. Dept. of the Interior, Minerals Management Service, Gulf of Mexico OCS Region, New Orleans, LA. 528 p.
Ochoa J, Sheinbaum J, Badan A, Candela J, Wilson D. 2001. Geostrophy via potential vorticity inversion in the Yucatan Channel. *Journal of Marine Research* 59:725–47.
Östlund HG, Rooth CGH. 1990. The North Atlantic tritium and radiocarbon transients 1972–1983. *Journal of Geophysical Research* 95:20147–65.
Östlund HG, Dorsey HG, Rooth CGH. 1974. GEOSECS North Atlantic radiocarbon and tritium results. *Earth and Planetary Science Letters* 23:69–86.
Ribbat B, Roether W, Münnich KO. 1976. Turnover of eastern Caribbean deep water from ^{14}C measurements. *Earth and Planetary Science Letters* 32:331–41.
Rivas D, Badan A, Ochoa J. 2005. The ventilation of the deep Gulf of Mexico. *Journal of Physical Oceanography* 35:1763–81.
Roemmich D. 1981. Circulation of the Caribbean Sea: a well-resolved inverse problem. *Journal of Geophysical Research* 86:7993–8005.
Romanou A, Chassignet EP, Sturges W. 2004. Gulf of Mexico circulation within a high-resolution numerical simulation of the North Atlantic Ocean. *Journal of Geophysical Research* 109: C01003. DOI: 10.1029/2003JC001770.
Rousset C, Beal LK. 2010. Observations of the Florida and Yucatan currents from a Caribbean cruise ship. *Journal of Physical Oceanography* 40:1575–81. DOI: 10.1175/2010JPO4447.1.
Rubin SI, Key RM. 2002. Separating natural and bomb-produced radiocarbon in the ocean: the potential alkalinity method. *Global Biogeochemical Cycles* 16:1105. DOI: 1029/2001GB001432.
Schmitz WJ. 2005. Cyclones and westward propagation in the shedding of anticyclonic rings from the Loop Current. In: Sturges W, Lugo-Fernandez A, editors. *Circulation in the Gulf of Mexico: Observations and Models. Geophysical Monographs* 161:241–61. Washington DC: American Geophysical Union.
Schroeder WW, Berner L Jr, Nowlin WD Jr. 1974. The oceanic waters of the Gulf of Mexico and Yucatan Strait during July 1969. *Bulletin of Marine Science* 24:1–19.
Sheinbaum J, Candela J, Badan A, Ochoa J. 2002. Flow structure and transport in the Yucatan Channel. *Geophysical Research Letters* 29:1040. DOI: 10.1029/2001GL013990.
Stuiver M. 1980. Workshop on ^{14}C data reporting. *Radiocarbon* 22(3):964–6.
Stuiver M, Polach HA. 1977. Discussion: reporting of ^{14}C data. *Radiocarbon* 19(3):355–63.
Stuiver M, Quay PD, Ostlund HG. 1983. Abyssal water carbon-14 distribution and the age of the world oceans. *Science* 219:849–51.
Sweeney C, Gloor E, Jacobson AJ, Key RM, McKinley G, Sarmiento JL, Wanninkhof R. 2007. Constraining global air-sea gas exchange for CO_2 with recent bomb ^{14}C measurements. *Global Biogeochemical Cycles* 21:GB2015. DOI: 10.1029/2006GB002784.
Toggweiler JR, Key RM. 2002. Ocean circulation: thermohaline circulation. In: Steel J, Thorpe S, Turekian K, editors. *Encyclopedia of Ocean Sciences*. London: Academic Press, Ltd. p 2941–7. 2001; also published in Holton JR, Pyle J, Curry JA, editors. *Encyclopedia of Atmospheric Sciences*. London: Academic Press. p 1549–55.
Wade TL, Sericano JL, Sweet ST, Knap AH, Guinasso NL. 2016. Spatial and temporal distribution of water column total polycyclic aromatic hydrocarbons (PAH) and total petroleum hydrocarbons (TPH) from the Deepwater Horizon (Macondo) incident. *Marine Pollution Bulletin* 103:286–93.
Weatherly GL, Wienders N, Romanou A. 2005. Intermediate-depth circulation in the Gulf of Mexico estimated from direct measurements. In: Sturges W, Lugo-Fernandez A, editors. *Circulation in the Gulf of Mexico: Observations and Models. Geophysical Monographs* 161:315–24. Washington DC: American Geophysical Union.
WHPO. 1994. *WHP Operations and Methods*. WOCE Hydrographic Office Report 91/1, as revised, WOCE Hydrographic Program Office, Woods Hole, MA.